

Band-gap renormalization of modulation-doped quantum wires

S. Sedlmaier,¹ M. Stopa,² G. Schedelbeck,¹ W. Wegscheider,^{1,*} and G. Abstreiter¹

¹Walter Schottky Institut, Am Coulombwall, D-85748 Garching, Germany

²Tarucha Mesoscopic Correlation Project, ERATO-JST, NTT Atsugi Research and Development Laboratory 3-1 Morinosato Wakamiya, Atsugi, Kanagawa 243-0198, Japan

(Received 10 January 2002; published 25 April 2002)

We measure the photoluminescence spectra for an array of modulation doped, *T*-shaped quantum wires as a function of the one-dimensional density n_e , which is modulated with a surface gate. We present self-consistent electronic structure calculations for this device which show a band-gap renormalization which, when corrected for excitonic energy and its screening, are largely insensitive to n_e and which are in quantitatively excellent agreement with the data. The calculations show that electron and hole remain bound up to $\sim 3 \times 10^6 \text{ cm}^{-1}$ and that, therefore, the stability of the exciton far exceeds the conservative Mott criterion, as determined from the Bethe-Salpeter equation.

DOI: 10.1103/PhysRevB.65.201304

PACS number(s): 78.66.-w, 71.15.Mb, 71.35.-y, 85.35.Be

Exchange and correlation (XC) in an electron gas formed in a semiconductor act to counter the direct Coulomb interaction by reducing the inter-particle overlap. For two component systems, such as the electron-hole plasma created in optical experiments, this effect tends to produce a band-gap renormalization (BGR) with increasing density n_e and/or n_h , reducing the energy of photons emitted upon recombination from the band edges.¹ Exciton formation further reduces the band gap but exciton binding is weakened by mobile charges so the trend with density opposes that of XC induced BGR. Investigations of the band gap, which has a pivotal dependence on the dimensionality of the system, is of interest both for its significance to optical technology and for the illumination it provides for the many-body problem. Consequently there are numerous experimental and theoretical studies of BGR which have focused on systems of successively lower dimension over the past several years.²⁻⁴

For one-dimensional systems, or quantum wires (QWRs), recent experimental and theoretical accounts have begun to clarify the often competing effects which result in density dependent changes to the observed photoluminescence energy.⁵⁻¹⁰ In general, BGR depends on the densities, n_e and n_h , of both components of the electron-hole plasma. Typically, however, research has concentrated on intrinsic samples wherein $n_e = n_h = n$. One difficulty with this approach has been that in order to vary n , increased photoexcitation power or time-resolved measurement as the excitation subsides have been required. Thus the observed spectra are complicated by highly nonequilibrium effects such as phase space filling. In this paper we present an experimental study of the evolution of the photoluminescence energy in a *doped* and *gated* *T*-shaped QWR, which allows modulation of n_e without increased photoexcitation. Our structure (see Fig. 1), fabricated via the cleaved edge overgrowth techniques¹¹ has appreciable advantages. It provides wires of high precision, with structural variations restricted to the monolayer regime. In addition, it permits the comparison of wire and quantum-well photoluminescence in a single sample.

To complement the measurements, we perform self-consistent electronic structure calculations within density-

functional theory (DFT) for this structure, using the local-density approximation (LDA) for XC, V_{xc} . The theoretical band-gap renormalization, which is usually calculated with many-body techniques, is equivalent to the *difference* between the LDA calculated band-gap and that calculated within a pure Hartree approximation, which omits the V_{xc} term. We have further calculated the effect of exciton formation and its screening on the band gap, using a simplified model potential with parameters derived from the DFT calculation.

Our principle result is that, as with experiments on two-component plasma in V-groove wires,⁶ the photoluminescence peak position is largely insensitive to density. The calculated screening of the exciton reduces the binding energy with a functional form that neatly cancels most of the XC induced BGR, predicting a recombination energy in excellent agreement with experiment. Additionally, the appearance of sharp structure in the photoluminescence (PL) data, indicating recombination from excitons localized at monolayer potential fluctuations, which gradually vanishes with increasing n_e , supports this BGR+exciton screening model. The calculation suggests that the exciton remains bound for very high density, also in agreement with Ref. 6, however the sharp structure disappears at much lower density, $n_e \sim 1 \times 10^6 \text{ cm}^{-2}$, indicating delocalization of the exciton. Alternatively, the disappearance of sharp structure could result from broadening due to density induced dephasing.

The cleaved edge overgrowth technique employed for our QWR structure has been described in detail elsewhere.¹¹ Our

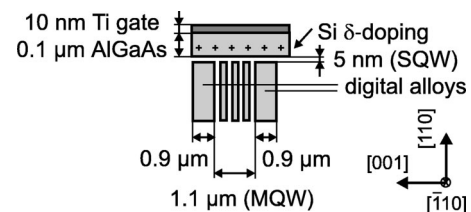


FIG. 1. Sample schematic showing the multiple, parallel *T*-shaped QWRs formed at the intersection of the edges of the multiple quantum wells (MQWs) with the single, modulation-doped quantum well (SQW) in the overgrowth layer (not true scale).

structure consists of 22 periods of (001)-oriented GaAs (5 nm)/Al_{0.32}Ga_{0.68}As (44 nm) quantum wells (multiple quantum wells, MQWs), grown between two digital alloys with 90 periods of GaAs (2 nm)/Al_{0.32}Ga_{0.68}As (8 nm) each. These digital alloys permit us to observe the PL from the overgrowth single quantum well (SQW), which is defined by growing along the [110]-crystal axis 5 nm GaAs, a 30 nm Al_{0.35}Ga_{0.65}As spacer, a silicon δ doping (*n*-modulation doping), and 70 nm Al_{0.35}Ga_{0.65}As. After both growth steps, 10 nm thick cap layers are added, which are not included in Fig. 1. *T*-shaped QWRs form with atomic precision at each 5×5 nm² wide intersection of the SQW with one of the multiple quantum wells.^{12,13}

To continuously vary the n_e in the QWRs and the SQW, we evaporate a 10 nm thick, semitransparent titanium gate on the surface of the overgrowth layer of a second set of samples. When the gate is grounded, the electron density in the SQW and in the QWRs are close to that of the ungated samples.

To maximize spatial resolution of the photoluminescence PL and photoluminescence excitation (PLE) spectroscopy, we focus the excitation beam of a tunable cw dye laser, pumped by an Ar-ion laser, with a microscope objective onto the sample, which is attached inside a cryostat to a copper block at the nominal temperature 5 K. On the sample, the diameter of the almost diffraction-limited laser spot amounts to about 800 nm full width at half maximum. A confocal imaging system guarantees that only PL limited to the laser spot region is detected.

For both ungated and gated samples, PLE spectra reveal that, due to an electron transfer from the doping layer into the SQW, an electron system is generated both in the SQW, between digital alloy and overgrowth spacer, and in the QWRs.

Exciting an ungated sample on the ($\bar{1}10$) surface, we are able to identify the QWRs PL because it is localized exactly and exclusively at the intersecting region of single and multiple quantum wells and is emitted at lower energy than the PL of the SQW and the MQWs.¹⁴ Of course, individual QWRs cannot be resolved, since they are spaced by 44 nm only, with respect to a spatial resolution of our instrument of about 800 nm, however the region of the wires (intersection of SQW and MQW) can be resolved from the region where only the SQW is present. In order to interpret the PL line shape of the *n*-modulation-doped *T*-shaped QWRs, we compare it with the line shape of *intrinsic* *T*-shaped QWRs, as shown in Fig. 2 (the curves are aligned horizontally so that the peaks coincide). Interface roughness, particularly in the (110)-oriented single quantum well,¹⁵ results in an inhomogeneously broadened, on average symmetric PL line of the intrinsic QWRs. The spectrally sharp peaks on the PL line are attributed to excitons localized at monolayer potential fluctuations.¹⁶ In the presence of free carriers as mentioned above, however, this signature of bound excitons vanishes, indicating exciton delocalization or density dependent damping. Furthermore, the asymmetric PL line shape indicates the formation of a 1D electron plasma in our modulation doped QWRs and band-to-band transitions between electrons of the Fermi sea and photogenerated holes. The Maxwell-

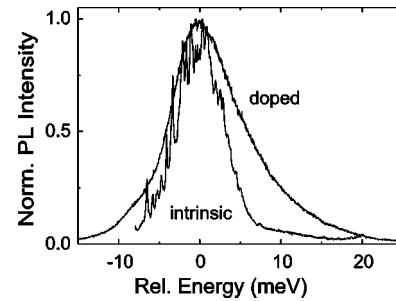


FIG. 2. Comparison between normalized PL line shapes of intrinsic and *n*-modulation doped *T*-shaped QWRs ($n \sim 1 \times 10^6$ cm⁻¹). Peaks aligned for comparison. Excitation and detection polarizations chosen parallel to the QWRs, consistent with Fig. 3. To detect only the QWRs PL and to avoid an overlap with the SQW PL, as in Fig. 3, excitation is performed on the (110) surface. Excitation power is 1 μ W, excitation energy is 1656 meV.

Boltzmann distribution of the photogenerated holes and the joint one-dimensional density of states $\sim 1/\sqrt{E}$ result in a decreasing recombination rate with increasing transition energy, assuming a constant transition-matrix element for *k*-conserving band-to-band recombinations.⁷ In *k* space, these transitions occur from the Γ point of the first Brillouin zone up to the Fermi wave vector. Thus, above the exciton recombination energy, which continues to mark the peak of the excitation, the wide high energy tail is clear evidence of the continuum in the conduction band resulting from the doping. Note that deviation from the $\sim 1/\sqrt{E}$ dependence of the joint DOS, which can result from Coulomb effects or inhomogeneities, will not change the qualitative nature of these conclusions.

We note that according to simulation results,¹⁷ only electrons in the first wire subband have maximum probability density at the *T* intersections. Electrons in the second subband are localized principally *between* pairs of *T*-intersections and have negligible overlap with the hole wave functions, which are more strongly localized at the junctions (due to higher effective mass). Therefore recombination from higher subbands is not expected to contribute to the asymmetry in the PL line shape.

For the gated sample (Fig. 3), excitation is performed from the (001)-sample surface. This permits us to observe simultaneously and compare the PL of the QWRs (peak on low energy side) and the SQW (high side) between digital alloy and overgrowth spacer. This also requires that for estimating the peak position of the wires we must deconvolve its line and the line from the quantum well. Applying a negative gate voltage relative to the electron system, the charge density in both the wires and the single quantum well is reduced. In Fig. 3, we have converted applied gate voltage into electron density per unit length for the QWRs and per unit area for the SQW. The bottom spectra of Fig. 3 displays the response for complete depletion as confirmed by a series of PLE measurements. Further increasing the depletion voltage changes neither the PL peak position, nor, qualitatively, the PL line shape; giving additional evidence that the electrons are totally depleted. With decreasing electron density, the PL lines of both the QWRs and the SQW narrow slightly, which

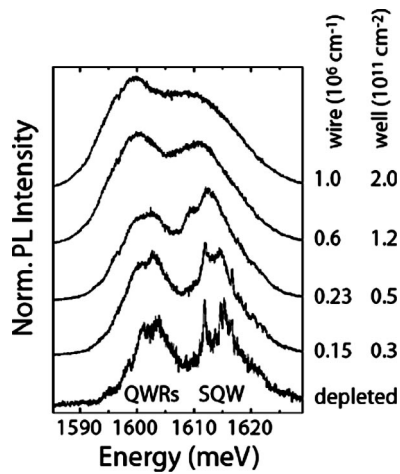


FIG. 3. Normalized and offset PL spectra of n -modulation doped QWRs and the SQW. We have increased the excitation power to 11 μ W because of the lower PL intensity in this geometry. The excitation energy is 1645 meV, the detected polarization lies parallel to the QWRs.

is consistent with a reduction of the Fermi wave vector for both the QWRs and the SQW. At low densities sharp peaks showing localized excitons are again evident, this time for the gated sample, in both the wire and the well photo response.

For the SQW the peak position, obtained by a simple line-shape fit, is redshifted by about 5–6 meV (Fig. 4) as the 2D electron density, N_e , is increased from zero to about $2 \times 10^{11} \text{ cm}^{-2}$ (this range, and the 1D density range from 0 to $1 \times 10^6 \text{ cm}^{-1}$ correspond to a gate voltage range of $[-5.2, 0]$ V). Correcting for the energy shift due to the quantum confined Stark effect,¹⁸ the residual shift, due to 2D BGR, amounts to about 5 ± 1 meV, in good agreement with earlier results for an n -modulation-doped quantum well.¹⁹ The indi-

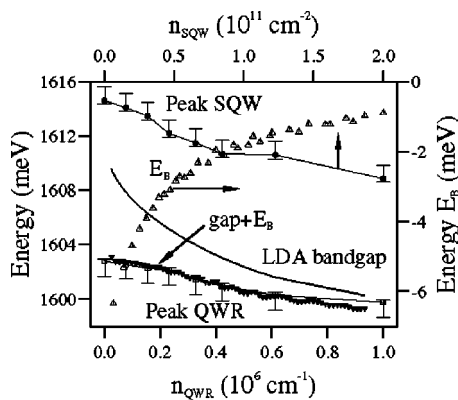


FIG. 4. Electron density dependence of the energetic peak positions of the QWRs (squares) and the SQW (dots, upper density scale), obtained by a simple line-shape fit of the spectra in Fig. 3. Error bars indicate the uncertainty in determining the peak positions. The calculated LDA band gap (heavy line) and the exciton binding energy E_b (hollow triangles, right scale) combine to produce the corrected gap (solid inverted triangles) which fits the data remarkably well. Note an overall offset is arbitrary due to the choice of the bulk band gap.

ated tolerance takes into account the uncertainty in determining the real PL peak position, as two PL lines overlap in Fig. 3.

The principle result of Fig. 4, however, is the strikingly weak variation of the peak position for the QWRs as n_e varies. The overall shift of only about 3 meV, when the electron density is increased from zero to about $1 \times 10^6 \text{ cm}^{-1}$, is similar to results found for wires with a two component plasma in high excitation.⁶

The observation is in excellent agreement with the variation of the band gap determined by the LDA calculation when the excitonic screening correction is included. The details of our calculation, which are based on a total free energy functional for the interacting wire-gate system²⁰ are discussed in a separate publication.¹⁷ In Fig. 4 we plot the variation of the translationally invariant band gap, the calculated exciton binding energy, and the combination of the two as a function of n_e . Clearly, without the screening of the exciton, the band-gap variation disagrees markedly with measurement. The variation of the exciton binding, however, is functionally nearly the inverse of the band-gap variation, with variation at low n_e strongest in both cases. The result is a close cancellation and a trend with n_e that recapitulates the data with remarkable fidelity.

Note that for densities above $\sim 5 \times 10^5 \text{ cm}^{-1}$ the second electron subband is expected to begin filling.¹⁷ However, our BGR calculations take all occupied subbands into account and the additional screening of the exciton binding energy due to electrons in higher subbands, which we do not include, should be negligible since the higher subband occupancy remains small in this range.

A similar cancellation of exciton binding energy and BGR has been derived recently by Das Sarma and Wang⁴ using the dynamically screened Bethe-Salpeter equation, for the case of a two-component, neutral plasma (i.e. for $n_e = n_h$). However one striking contrast between our results and those of Ref. 4 is that, up to our highest density $n_e = 3 \times 10^6 \text{ cm}^{-1}$, we find that the electron and hole *remain bound*, whereas those authors find a merging of the exciton with the continuum, a so-called “Mott transition,” in the range of $0.3 \times 10^6 \text{ cm}^{-1}$. Previous calculations employing the statically screened Bethe-Salpeter equation have determined a Mott density of $\sim 7 \times 10^5 \text{ cm}^{-1}$ in quasi-1D.³ The robustness of the exciton revealed in our calculations emerges from the requirement of orthogonality between the free, screening electrons and those bound to the hole; a constraint which is not maintained in the many-body calculation.

We note that the density functional method includes automatically the full *non linear* effects of screening, whereas many-body calculations often assume linear screening and hence are not valid in the low density limit. It is in the low density regime where BGR and the excitonic binding energy change most rapidly with density. The strong tendency to cancel suggests a fundamental connection between the two processes. The exchange portion of the energy, which dominates V_{xc} at low density, varies as $-\rho^{1/3}$. Therefore a $+\rho^{1/3}$ dependence for the screened exciton interaction is suggested, although we do not have a fundamental argument for this.

In conclusion, we have presented photoluminescence measurements of a modulation-doped and surface gated *T*-shaped quantum wire which exhibit a weak dependence of the peak position on the density of conduction-band electrons in the wire. We have also reported on density-functional calculations for the structure which show a band-gap renormalization of ~ -10 meV over the range of

measured densities. A calculation of the excitonic binding energy and its screening shows a complementary trend to the BGR such that the combined results are largely insensitive to n_e and agree well with the observed line peak. Finally, we find that while the exciton binding weakens with density, it nonetheless remains bound up to $n_e = 3 \times 10^6$ cm⁻³, suggesting an excitonic stability well in excess of the Mott criterion.

*Permanent address: Universität Regensburg, 93040 Regensburg, Germany. Email: stopa@tarucha.jst.go.jp

- ¹For reviews, see H. Kalt, *Optical Properties of III-V Semiconductors* (Springer-Verlag, Berlin, 1996); H. Haug and S.W. Koch, *Quantum Theory of the Optical and Electronic Properties of Semiconductors* (World Scientific, Singapore, 1993).
- ²R. Rinaldi *et al.*, Phys. Rev. B **59**, 2230 (1999); S. Schmitt-Rink, D. Chemla, and D.A.B. Miller, Adv. Phys. **38**, 89 (1989); R. Cingolani and K. Ploog, *ibid.* **40**, 535 (1991); R. Zimmermann, K. Kilimann, W.D. Kraeft, D. Kremp, and G. Röpke, Phys. Status Solidi B **90**, 175 (1978).
- ³S. Nojima, Phys. Rev. B **51**, 11 124 (1995); F. Rossi and E. Molinari, Phys. Rev. Lett. **76**, 3582 (1996); S. Das Sarma, R. Jalabert, and S.R. Eric Yang, Phys. Rev. B **39**, 5516 (1989); F. Tassone and C. Piermarochi, Phys. Rev. Lett. **82**, 843 (1999).
- ⁴S. Das Sarma and D.W. Wang, Phys. Rev. Lett. **84**, 2010 (2000).
- ⁵W. Wegscheider, L.N. Pfeiffer, M.N. Dignam, A. Pinczuk, K.W. West, S.L. McCall, and R. Hull, Phys. Rev. Lett. **71**, 4071 (1993).
- ⁶R. Ambigapathy, I. Bar-Joseph, D.Y. Oberli, S. Haacke, M.J. Brasil, F. Reinhardt, E. Kapon, and B. Deveaud, Phys. Rev. Lett. **78**, 3579 (1997).
- ⁷R. Cingolani, R. Rinaldi, M. Ferrara, G.C. La Rocca, H. Lage, D. Heitmann, K. Ploog, and K. Halt, Phys. Rev. B **48**, 14331 (1993).

- ⁸Ben Yu-Kuang Hu and S. Das Sarma, Phys. Rev. Lett. **68**, 1750 (1992); Phys. Rev. B **48**, 5469 (1993).
- ⁹S. Benner and H. Haug, Europhys. Lett. **16**, 579 (1991); B. Tantar, J. Phys.: Condens. Matter **8**, 5997 (1996).
- ¹⁰E.H. Hwang and S. Das Sarma, Phys. Rev. B **58**, R1738 (1998).
- ¹¹L. Pfeiffer, K.W. West, H.L. Stormer, J.P. Eisenstein, K.W. Baldwin, D. Gershoni, and J. Spector, Appl. Phys. Lett. **56**, 1697 (1990).
- ¹²S. Glutsch, F. Bechstedt, W. Wegscheider, and G. Schedelbeck, Phys. Rev. B **56**, 4108 (1997).
- ¹³A.R. Goñi, L.N. Pfeiffer, K.W. West, A. Pinczuk, H.U. Baranger, and H.L. Stormer, Appl. Phys. Lett. **61**, 1956 (1992).
- ¹⁴T. Someya, H. Akiyama, and H. Sakaki, J. Appl. Phys. **79**, 2522 (1996).
- ¹⁵R.D. Grober, T.D. Harris, J.K. Trautman, E. Betzig, W. Wegscheider, L. Pfeiffer, and K. West, Appl. Phys. Lett. **64**, 1421 (1994).
- ¹⁶J. Hasen, L.N. Pfeiffer, A. Pinczuk, K.W. West, and B.S. Dennis, Nature (London) **390**, 54 (1997).
- ¹⁷M. Stopa, Phys. Rev. B **63**, 195312 (2001).
- ¹⁸G. Bastard, *Wave Mechanics Applied to Semiconductor Heterostructures* (Les Ulis Cedex, Les Éditions de Physique, Paris, 1998), p. 239.
- ¹⁹C. Delalande, G. Bastard, J. Orgonasi, J. Brum, H. Liu, and M. Voos, Phys. Rev. Lett. **59**, 2690 (1987).
- ²⁰M. Stopa, Phys. Rev. B **54**, 13767 (1996).